Magnetic anisotropy in symmetric magnetic colloidal quantum dots doped with few Mn^{2+} impurities

Shun-Jen Cheng
Department of Electrophysics, National Chiao Tung University, Hsinchu 300, Taiwan, Republic of China
(Received 6 April 2009; revised manuscript received 11 May 2009; published 1 June 2009)

We present numerical exact diagonalization studies of the magnetism in magnetic II-VI colloidal semiconductor quantum dots charged with controlled number of electrons coupled to few magnetic-ion (Mn^{2+}) dopants. The interplay between various relevant spin interactions and the discrete nature of Mn^{2+} spin distribution is shown to be essential in the magnetism of few Mn^{2+}-doped quantum dots. An interesting revealed feature is the existence of pronounced magnetic anisotropies in *symmetric* magnetic quantum dots, which are related to the orbital quenchings induced by electron-Mn spin interactions. The orbital quenching effects further lead to significant deviations of the magnetizations of randomly Mn-doped dots from the standard Brillouin-function descriptions.

DOI: 10.1103/PhysRevB.79.245301 PACS number(s): 68.65.Hb, 75.20.−g, 75.75.+a

I. INTRODUCTION

Recent progress in the fabrication of magnetic-ion-doped semiconductor quantum dots (QDs) (Refs. 1–6) has stimulated a broad interest in exploring their application potential in spintronics and fundamental physical properties.[7–26] The spin interactions involving carriers and/or magnetic dopants are known to be essential in the magnetic properties of magnetically doped semiconductors.[27] For magnetic semiconductor bulks or thin films containing a large number of magnetic-ion dopants,[28] they are usually simplified to effective continuous fields in mean-field theory.[29,30] However, the number of magnetic ions in a magnetic QD is small (typically only 10^0-10^1) and the discreteness of the spatial distribution of magnetic dopants should affect the magnetic behavior significantly.[10]

In this work we present exact diagonalization (ED) studies of the magnetism in charged II-VI CdSe colloidal semiconductor nanocrystal quantum dots (NCQDs) doped with few divalent magnetic ions (Mn^{2+}) interacting with controlled number of charging electrons. With the high controllability of quantum confinement (size and shape)[31] and magnetic impurity dopings,[1] magnetic NCQDs provide an excellent test bed for studying the various spin interactions and their interplay with other controlled dot parameters, e.g., the size of dot, the number of resident electrons, the density, and the spatial distribution of magnetic-ion dopants and external fields. The numerical ED approach employed here allows us to precisely calculate the energy spectra and magnetic properties of interacting charged NCQDs doped with few Mn^{2+} ions, with the full consideration of all relevant electron-electron (e-e), electron-Mn (e-Mn), and Mn-Mn spin interactions and the discrete nature of magnetic-ion spin distribution.

One of the most striking features revealed by our ED studies is the existence of magnetic anisotropies (MAs) in few Mn-doped *symmetric* NCQDs. The physical origins of the MAs are attributed to the magnetic-ion-induced orbital quenchings, which depend on the number of resident electrons and the orientations of applied fields with respect to the spatial distribution of magnetic ions. Furthermore, the orbital quenching effects lead also to significant deviations of the magnetic behaviors of Mn-doped NCQDs from the standard Brillouin-function descriptions.

II. MODEL HAMILTONIAN AND NUMERICAL APPROACH

The Hamiltonian of a magnetic semiconductor quantum dot charged with interacting electrons coupled to magnetic ions (Mn^{2+}) at zero magnetic field is written as[10]

$$H_0 = H_e + H_{\text{Mn}} + H_{e\text{-Mn}}, \tag{1}$$

where H_e is the Hamiltonian of interacting electrons in a Mn-free dot, H_{Mn} is that of the subsystem of magnetic ions, and $H_{e\text{-Mn}}$ describes the interactions between electrons and Mn ions. In the basis of single-electron bound orbitals of dot, H_e is written as $H_e=\Sigma_{i\sigma}\epsilon_i c^+_{i\sigma}c_{i\sigma}+\frac{1}{2}\Sigma_{ijkl;\sigma\sigma'}V_{ijkl}c^+_{i\sigma}c^+_{j\sigma'}c_{k\sigma'}c_{l\sigma}$, where the subscripts i,j,k,l label the bound orbitals, $\sigma=\uparrow/\downarrow$ denotes the spin of electron with $s_z=\frac{1}{2}/-\frac{1}{2}$, $c^+_{i\sigma}$ ($c_{i\sigma}$) is the creation (annihilation) operator for the electron in the orbital $|i;\sigma\rangle$, ϵ_i is the kinetic energy of a single electron, and $V^{e\text{-}e}_{ijkl} \equiv \int\int d^3r_1 d^3r_2 \phi^*_i(\vec{r}_1)\phi^*_j(\vec{r}_2)(e^2/4\pi\kappa|\vec{r}_1-\vec{r}_2|)\phi_k(\vec{r}_2)\phi_l(\vec{r}_1)$ are Coulomb matrix elements, where ϕ_i is the wave function of an electron in $|i;\sigma\rangle$, e is the elementary charge of electron, and κ is the dielectric constant of dot material. In this work, the hard-wall sphere model for the confining potential of spherical NCQDs is taken.[32,33] Accordingly, the wave function and the eigenenergy of a single electron in a symmetric NCQD are explicitly expressed by $\phi_{nlm\sigma}(\vec{r}) = \sqrt{2/a^3}[J_l(\frac{\alpha_{nl}}{a}r)/J_{l+1}(\alpha_{nl})]Y_{lm}(\theta,\phi)$ and $\epsilon_{nl}=(\hbar^2\alpha^2_{nl})/(2m^*a^2)$, respectively, where a is the radius of spherical dot, m^* is the effective mass of electron, n is the principal quantum number, l is the angular momentum, m is the z component of angular momentum, $J_l(r)$ is the spherical Bessel function, α_{nl} is the nth zero of J_l, and $Y_{lm}(\theta,\phi)$ is the spherical Harmonic function. Throughout this work, $m^*=0.15m_0$ and $\kappa=8.9\epsilon_0$ are taken for CdSe QDs.

The Hamiltonian of the subsystem of Mn ions is described by the antiferromagnetic (AF) Mn-Mn interactions, $H_{\text{Mn}}=-\frac{1}{2}\Sigma_{p\neq q}J_{\text{Mn-Mn}}(R_{IJ})\vec{I}_p\cdot\vec{I}_q$, where $\vec{I}_p$ ($\vec{I}_q$) denotes the spin

of the pth (qth) Mn^{2+} impurity at position $\vec{R}_p$ ($\vec{R}_q$) and $J_{\text{Mn-Mn}}(R_{pq})=J^{(0)}_{\text{Mn-Mn}}\exp\{-\lambda[(R_{pq}/a_0)-1]\}<0$, where $R_{pq}\equiv|\vec{R}_p-\vec{R}_q|$, $J^{(0)}_{\text{Mn-Mn}}=-0.5$ meV, $a_0=0.55$ nm, and $\lambda=5.1$.[10,17] The Mn-Mn interactions are short ranged and sensitively depend on the distances between Mn ions, R_{pq}, which are associated with the density and distribution of Mn ions.

The electron and Mn subsystems are coupled via the ferromagnetic (FM) contact interactions,

$$H_{e\text{-Mn}}=-\tfrac{1}{2}\sum_q\sum_{i,i'}J^{e\text{-Mn}}_{ii'}(\vec{R}_q)[(c^+_{i'\uparrow},c_{i\uparrow}-c^+_{i'\downarrow},c_{i\downarrow})I^z_q+c^+_{i'\downarrow},c_{i\uparrow}I^+_q+c^+_{i'\uparrow},c_{i\downarrow}I^-_q],$$

where I^z_q is the z component of Mn spin, $I^\pm_q\equiv I^x_q\pm iI^y_q$, and the magnetic coupling constants are defined as $J^{e\text{-Mn}}_{ii'}(\vec{R}_q)\equiv J^{(0)}_{e\text{-Mn}}\psi^*_i(\vec{R}_q)\psi_{i'}(\vec{R}_q)$. Throughout this work, the e-Mn coupling parameter $J^{(0)}_{e\text{-Mn}}=10.8$ meV $\text{nm}^3>0$ is taken for substitutional Mn ions in CdSe bulk.[10,17] In Mn:CdSe QDs, the spin interactions between quantum-confined electrons and Mn ions are actually determined by the *effective*-Mn coupling $J^{e\text{-Mn}}_{ii'}=J^{(0)}_{e\text{-Mn}}\psi^*_i(\vec{R}_q)\psi_{i'}(\vec{R}_q)\propto a^{-3}$, which depends on dot size, positions of Mn ions, and involved electronic orbitals.[17]

Applying an external magnetic field $\vec{B}=(0,0,B)$ yields the following B-dependent terms additional to H_0,

$$H_B=\sum_n(g_{\text{Mn}}\mu_BB)I^z_n+\sum_{i\sigma}(\mu^*_BB)m_ic^+_{i\sigma}c_{i\sigma}+\sum_{i\sigma}(g_e\mu_BBs_z)c^+_{i\sigma}c_{i\sigma},\quad(2)$$

where the first term is the spin Zeeman energies of Mn ions, the second (last) one is the orbital (spin) Zeeman energies of electrons, $\mu_B\equiv\hbar e/2m_0$ ($\mu^*_B\equiv\hbar e/2m^*$) is the bare (effective) Bohr magneton, and $g_e=1.2$ ($g_{\text{Mn}}=2.0$) is the g factor of electron (Mn). Diamagnetic terms are neglected here because of the small sizes of NCQDs.[17] Generally, the magnetic moments from the first two terms in Eq. (2) are more significant than the one from electron spins because of large orbital moments of electrons ($\mu^*_B\gg\mu_B$ because $m^*\ll m_0$) and large spin of Mn ($I=5/2$). Thus, the magnetization of a Mn-free QD mainly depends on the orbital arrangement of electrons, which are determined by the e-e Coulomb interactions and Zeeman energies. Nevertheless, the spin interactions involving electron spins are essential in the magnetism of magnetic QDs which contain magnetic ions. In the presence of Mn ions, electrons could favor to fill the orbitals that are directly coupled to the magnetic ions to gain more energies from the FM e-Mn interactions, in competition with the effect of orbital Zeeman energies. Furthermore, magnetic ions tend to order their spins via the simultaneous contact spin interactions with electrons. However, the AF interactions between Mn ions, opposite to the effects of FM e-Mn interactions, tend to minimize the total spin of Mn's. The competition between the various spin interactions and B-dependent Zeeman energies result in complex and interesting features of the magnetism of magnetically doped QDs. Table I shows the energy scales of the relevant spin interactions and Zeeman energies in Mn-doped NCQDs at $B=1$ T.

TABLE I. Relevant energy scales of Mn-doped nanocrystal quantum dots.

Physical quantities	Energy scale (meV)
Single-electron energy quantization	$>10^2$
Direct Coulomb interaction	10^2
Exchange Coulomb interaction	10^1
Electron-Mn interaction	10^0
Mn-Mn interaction (nearest neighbor)	10^0
Orbital Zeeman energy (electron) for $B=1$ T	$10^{-1}-10^0$
Spin Zeeman energy (Mn) for $B=1$ T	$10^{-1}-10^0$
Spin Zeeman energy (electron) for $B=1$ T	$10^{-2}-10^{-1}$

The energy spectra of multiply charged magnetic NCQDs are calculated by using exact diagonalization techniques.[10,17] Taking the product of the *all* possible Mn spin configurations and selected electron configurations as basis, the matrix for the full Hamiltonian $H=H_0+H_B$ is constructed and the magnetoenergy spectrum of a multiply charged magnetic NCQDs is obtained by performing direct diagonalization for the matrix. Convergence of numerical results is tested by increasing number of configurations. The magnetization of N_e-electron dot at temperature T is calculated by the definition $M=\frac{1}{\beta}(\frac{\partial\ln Z}{\partial B})_T$, where $\beta\equiv1/(k_BT)$ and $Z=\Sigma_i\exp[-E_i(N_e;B)\beta]$ is the canonical ensemble equilibrium partition function.[17,34]

III. RESULTS AND DISCUSSION

A. Magnetizations as functions of B and N_e

Let us first examine charged magnetic dots doped with two long-ranged Mn ions. Figure 1(a) [Fig. 1(c)] shows the calculated magnetizations versus applied magnetic fields $\vec{B}=(0,0,B)$ of multiply charged ($N_e=1-8$) CdSe NCQDs of radius $a=3$ nm doped with two Mn ions positioned at $R_1=(a/2,0,0)$ and $R_2=(-a/2,0,0)$ on the x-y plane [$R_1=(0,0,a/2)$ and $R_2=(0,0,-a/2)$ on the y-z plane], respectively, at the low temperature $kT=0.1$ meV. At small fields $B\ll1$ T, where the p-orbital Zeeman splittings are smaller than the thermal energy and mean e-Mn interactions, $\langle H_z\rangle\equiv E_z\ll kT$, $J_{e\text{-Mn}}$, the magnetizations of the Mn-doped NCs follow Curie's law, showing rapid and linear increases with B. The increasing magnetizations reach their saturated values as $B\gtrsim5$ T (depending on N_e), where $E_z\gg kT$, $J_{e\text{-Mn}}$. In spite of large-orbital Zeeman energies E_z, the orbital arrangement of electrons in the small NCQDs in the high fields, $5\text{ T}\lesssim B\lesssim10$ T, follows Hund's rules because of strong e-e Coulomb interactions [$V_{e\text{-}e}\gg E_z$ (see Table I)]. The high-field magnetizations, which are determined mainly by the orbital moments of electrons, thus show a similar N_e dependence to that of total orbital angular momentum of electrons according to Hund's rules [see the insets of Figs. 1(a) and 1(c)].[35] Remarkably, the optimal magnetism is observed in the charged NCs with $N_e=3,4,6,7$ instead of the dots with half-filled shells ($N_e=5$) with maximum total spin but vanishing total orbital angular momentum as expected by mean-field

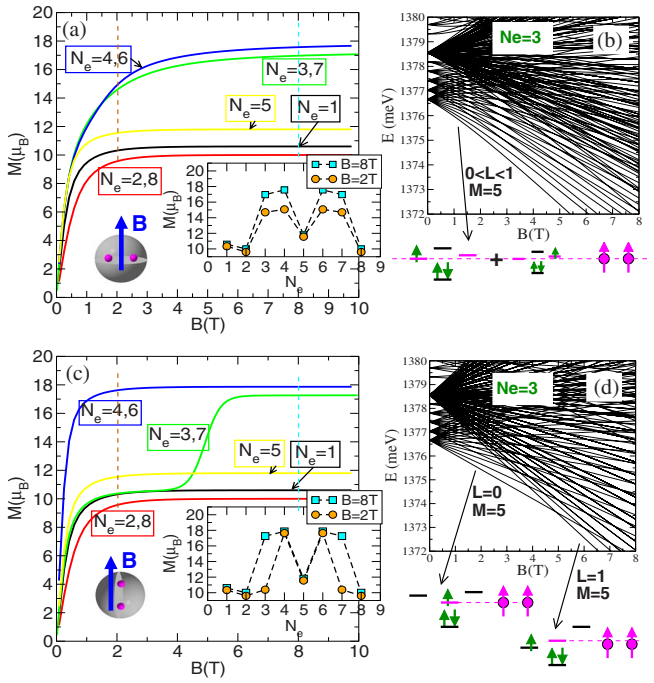

FIG. 1. (Color online) (a) The magnetizations versus applied magnetic fields $\vec{B}=(0,0,B)$ of multiply charged ($N_e=1-8$) NCQDs of radius $a=3$ nm doped with two Mn ions positioned at $(\pm a/2,0,0)$ at low temperature $kT=0.1$ meV. The inset shows the magnetizations of the charged dots as a function of N_e at $B=2$ and 8 T. (b) The low-lying magnetoenergy spectrum of the two Mn^{2+}-doped NCQD with $N_e=3$ in (a). (c) The magnetizations vs $\vec{B}=(0,0,B)$ of various multiply charged NCs doped with two Mn ions at $(0,0,\pm a/2)$. (d) The magnetoenergy spectrum of the two Mn^{2+}-doped NCQD with $N_e=3$ in (c).

theory[16] because of the dominant electron orbital moments ($\mu_B^* \gg \mu_B$) in the strongly quantized dots.[17]

B. Magnetic-ion-induced magnetic anisotropies

In the intermediate field regime (1 T$\lesssim B \lesssim$5 T), where $kT \ll E_z \lesssim J_{e\text{-Mn}}$, the orbital Zeeman energies and e-Mn spin interactions are energetically comparable and their interplay might lead to interesting features of magnetism. An interesting finding revealed by the ED studies is the existence of MAs in multiply charged NCQDs doped with few Mn ions (even though the shapes of the dots are perfectly symmetric). The MAs are especially pronounced in the dots with singly charged shell, e.g., triply charged ($N_e=3$) dots, where the single electron on the p-shell subjects to only weak intershell Coulomb interactions.

The magnetizations of $N_e=3$ NCQDs doped with two Mn ions are found to be significantly suppressed as applied magnetic fields of intermediate strength (2 T$\lesssim B \lesssim$5 T) are along the axis connecting the two magnetic ions, as shown in comparing Fig. 1(c). In the intermediate B regime where $E_z < J_{e\text{-Mn}}$, the sole p-shell electron in the $N_e=3$ magnetic NCQD of Fig. 1(c) is prone to fill the p_0 orbital of $l_z=0$ that is directly coupled to the two Mn ions for gaining more energy from the e-Mn couplings ($J_{e\text{-Mn}}$), even though the p_{-1} orbital of $l_z=-1$ is also lowered by E_z. Such a magnetic-ion-induced orbital quenching leads to a vanishing orbital magnetic moment in the intermediate B regime. Further increasing the magnetic field to $B \gtrsim 5$ T, where $E_z \gtrsim J_{e\text{-Mn}}$, the electron occupying the p_0 orbital transfers back to p_{-1} orbital and the magnetization of the dot abruptly increases. Figure 1(d) shows the energy spectrum versus B of the $N_e=3$-charged NCQD doped with two Mn^{2+} ions for Fig. 1(c) and schematically presents the main e-Mn configurations of the ground states.

By contrast, such a kind of magnetic-ion-induced orbital quenching does not occur in the triply charged magnetic dots in the magnetic fields perpendicular to the plane where Mn ions are located [see Fig. 1(a)]. In the situation, both of the $p_{l_z=+1}$ and $p_{l_z=-1}$ orbitals are coupled to the two magnetic ions but only the energy level of $p_{l_z=-1}$ orbital is further lowered by E_z. It turns out that the single p-shell electron stays in the $p_{l_z=-1}$ orbital mostly but could be slightly scattered to the $p_{l_z=+1}$ orbital by the magnetic impurities, and the $N_e=3$ magnetic QD exhibits a finite orbital moment that is only slightly weaker than the full $l=1$ moment. Figure 1(b) shows the energy spectrum versus B of the $N_e=3$-charged NCQD with two Mn^{2+} ions for Fig. 1(a) and the main configurations of the ground states. Comparing Figs. 1(a) and 1(c), the magnetization of the two Mn-doped NCQDs charged with $N_e=3$ is shown to be optimal as the applied fields $\vec{B}$ are perpendicular to the axis connecting the two Mn ions. Apparently, such MAs are directly associated with the discreteness of Mn distribution, which is however disregarded in widely used mean-field theory.[15,16]

C. Quantum size effects

We next examine the quantum size and charging effects on the MAs. Figures 2(a)–2(f) show the calculated magnetizations of $N_e=3$- and $N_e=4$-charged NCs of various radii $a=2,3,5$ nm doped with two Mn ions at $(\pm a/2,0,0)$ on the x-y plane and under the magnetic fields in the two directions, $\vec{B}_{\parallel}=(B,0,0)$ or $\vec{B}_{\perp}=(0,0,B)$. With reducing the dot size, the MAs become even more pronounced and persist over a wider range of B because the e-Mn spin interactions are significantly enhanced by the quantum confinements of QDs. The B ranges of the MAs reflect the strength of $J_{e\text{-Mn}}$. The quantum size effects however do not improve the magnetism. At a fixed magnetic field, the magnetizations actually decrease with decreasing NC sizes because the orbital quenchings are more significant in smaller QDs.

Unlike the cases of $N_e=3$, the optimal magnetizations of two Mn-doped NCQDs with $N_e=4$ electrons occur as the applied magnetic fields $\vec{B}_{\parallel}$ are along the axis (x axis) connecting the two Mn's. In the situation, one of the two p-shell electrons occupies the p_y-p_z-hybridized orbital of $l_x=-1$ and the other one stably stays in the p_x orbital of $l_x=0$ that is directly coupled to the two Mn's. Without experiencing impurity scatterings, the former electron freely moves on the Mn-free y-z plane and provides a full $l=1$ orbital moment. Turning the magnetic field to the $\vec{B}_{\perp}$ in the z direction, the two p-shell electrons are transferred to the p_x-p_y hybridized

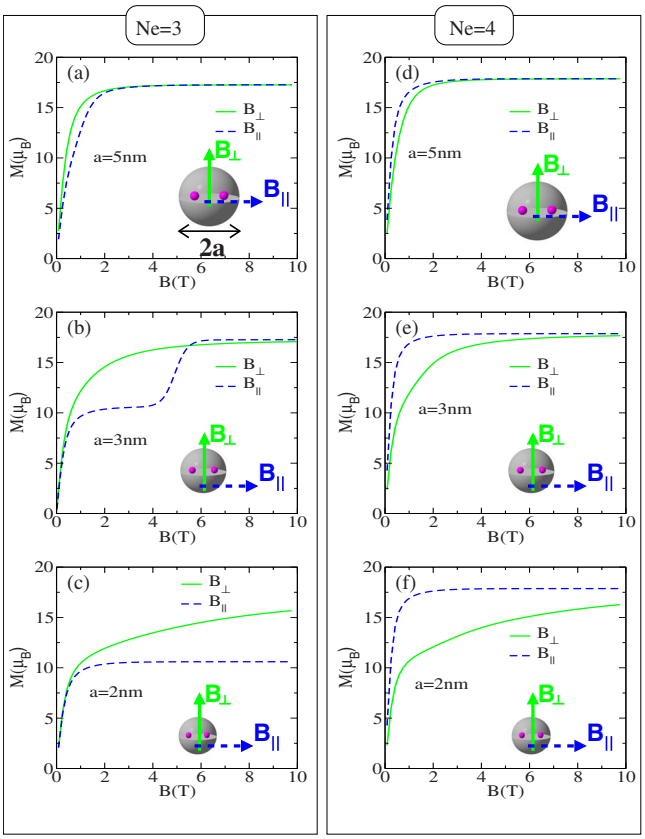

FIG. 2. (Color online) The size effects on the magnetic anisotropies of magnetically doped NCQDs. [(a)–(c)] The magnetizations vs $\vec{B}_{\parallel}=(B,0,0)$ and $\vec{B}_{\perp}=(0,0,B)$ of $N_e=3$-charged NCQDs of various radii ($a=2,3,5$ nm) with two long-ranged Mn ions at $(\pm a/2,0,0)$. [(d)–(f)] Same as [(a)–(c)] but for $N_e=4$.

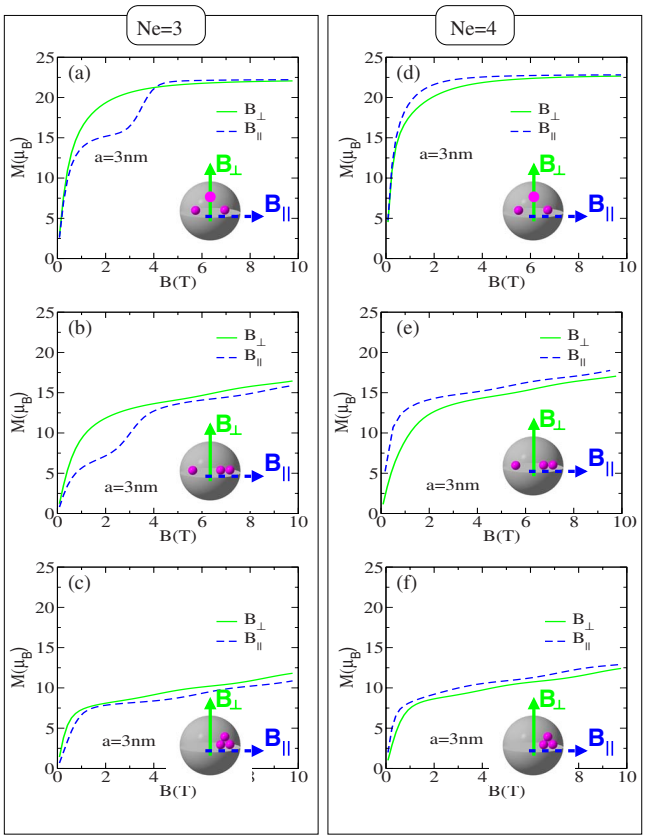

FIG. 3. (Color online) The effect of the spatial distribution of Mn ions on the magnetic anisotropies of magnetically doped NCQDs. [(a)–(c)] The magnetizations vs $\vec{B}_{\parallel}=(B,0,0)$ and $\vec{B}_{\perp}=(0,0,B)$ of $N_e=3$-charged NCQDs of radius $a=3$ nm with three Mn ions at various positions (see the schematics). [(d)–(f)] Same as [(a)–(c)] but for $N_e=4$.

orbital of $l_z=-1$ and the p_z orbital of $l_z=0$. The former electron moving on the x-y plane is likely scattered by the two Mn ions positioned on the plane and the electron orbital moment is reduced to be weaker than that of $l=1$.

D. Interplay between various spin interactions and the discreteness of Mn^{2+} spin distributions

The magnetic anisotropy could be expected also in charged QDs with single Mn ions.[17] However, increasing more Mn ions in a QD yields a rich interplay between various spin interactions, Zeeman energies, and Coulomb interactions because of more varieties of Mn distributions. To further identify how the distribution of magnetic-ion dopants affects the magnetic properties of few Mn-doped NCQD, we consider different magnetic NCQDs containing long-ranged Mn ions and/or short-range interacting Mn clusters. Figure 3(a)–3(f) show the magnetizations of $N_e=3,4$-charged NCQDs of radius 3 nm doped with three Mn's at various positions under magnetic fields perpendicular or parallel to the x-y plane, $\vec{B}_{\perp}$ or $\vec{B}_{\parallel}$. Here, we consider only the magnetic ions positioned at $(\pm a/2,0,0)$, $(0,\pm a/2,0)$, and $(0,0,\pm a/2)$ or (0,0,0) in QDs of radius a. In Figs. 1–4, NCQDs are schematically depicted by larger gray spheres and the positions of Mn ions in the NCQDs are indicated by small red-filled circles distributed in the spheres. Pronounced MAs are observed in the intermediate B regime as the magnetic NCQDs contain long-ranged Mn ions [Figs. 3(a), 3(b), 3(d), and 3(e)]. For the NCQDs containing only short-range interacting Mn clusters [Figs. 3(c) and 3(f)], the magnetizations are weak and the MAs become ambiguous.

Experimentally, probing such MAs in individual NCQDs is quite challenging. Nevertheless, the MAs may cause observable significant deviations of the magnetizations of randomly Mn-doped NCQD ensembles from the standard Brillouin-function description for the magnetizations of ideal paramagnets. According to the theory of atomic magnetism, the magnetization of an isolated paramagnet of total three Mn spin $I=15/2$ (a noninteracting electron of the effective mass $m^*=0.15m_0$ with angular momentum $l=1$) is explicitly described by $M_{15/2}=(\frac{15}{2})g_{\mathrm{Mn}}\mu_B B_{15/2}(15g_{\mathrm{Mn}}\mu_B B/2kT)$ [$M_1^*=\mu_B^* B_1(\mu_B^* B/kT)$, where B_J is Brillouin function]. Thus, the magnetization of a *noninteracting* magnetic NCQD with decoupled three Mn ions and a p-shell electron should follow $M=M_{15/2}+M_1^*$, as indicated by the dashed line in Fig. 4. Figure 4 shows the magnetizations of more $N_e=3$-charged CdSe NCQDs doped with three Mn^{2+} ions at various positions. In general, the magnetizations as functions of B of the most magnetic NCQDs shown in Fig. 4 deviate significantly

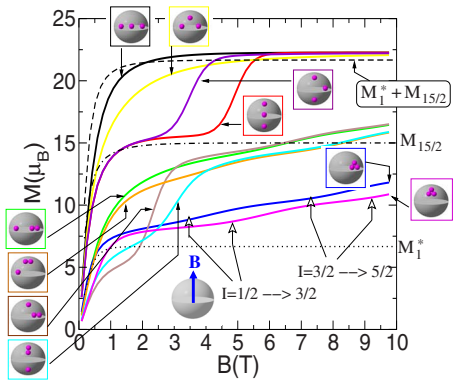

FIG. 4. (Color online) Calculated magnetizations versus applied field $\vec{B}=(0,0,B)$ of various three Mn-doped CdSe NCQDs of radius $a=3$ nm charged with three electrons. Dotted line: the magnetization $M_1*=\mu_B^* B_1(\mu_B^* B/kT)$ provided by the magnetic orbital moment of an electron of effective mass $m^*=0.15$ on a $l=1$ orbital, where B_J is Brillouin function. Dotted-dashed line: the magnetization $M_{15/2}=(\frac{15}{2})g_{\mathrm{Mn}}\mu_B B_{15/2}(15g_{\mathrm{Mn}}\mu_B B/2kT)$ provided by the magnetic moment of a three Mn spin $I=15/2$. Dashed line: the total magnetization $(M=M_1*+M_{15/2})$ of a *noninteracting* magnetic NCQD containing a single *p*-shell electron and three Mn ions.

from the Brillouin function $M=M_{15/2}+M_1^*$ (dashed line in Fig. 4). The magnetizations of the three Mn-doped NCQDs are generally lower than that of a noninteracting dot $(M=M_{15/2}+M_1^*)$ and fall into three groups according to the high-field magnetizations, associated with the number of short-ranged Mn ions.

The magnetization deviations from the standard Brillouin-function behavior are directly related to various relevant spin interactions. The significant suppression of magnetization in the intermediate B regime is attributed to the orbital quenchings associated with the FM e-Mn interactions, as pointed out previously. By contrast, the AF Mn-Mn interactions in the short-ranged Mn clusters are responsible for the substantially reduced magnetization over a wide range of B. The strong AF Mn-Mn interactions in the three Mn-cluster yield the magnetic ground states of the minimum total spin of Mn's $(I_{\mathrm{tot}}=1/2)$ at zero fields. The small Mn spins make the e-Mn spin interactions very weak and the magnetizations insensitive to the orientations of magnetic fields. Further increasing B, the increasing orbital Zeeman splittings lower the energies of high I_{tot} states, and eventually the ground states of the magnetic QD are switched to the ones with higher I_{tot} at certain B fields. As a result, the magnetic NCQDs undergo a series of ground-state transitions from low-spin states to high-spin states $(I_{\mathrm{tot}}=1/2\rightarrow 3/2, 3/2\rightarrow 5/2,\ldots)$ with increasing B, leading to the slight rippling features of the magnetizations as functions of B.[14] Basically, the MAs revealed in this work are mainly associated with the FM e-Mn interactions. The AF Mn-Mn interactions in Mn clusters minimize the total spin of Mn's and do not make significant contributions to the MAs. However, the combined effects of the orbital quenchings associated with the FM e-Mn interactions and the magnetic ground-state transitions due to the AF Mn-Mn interactions result in the complex magnetization features of randomly Mn^{2+}-doped quantum dots, which are significantly deviated from the standard paramagnetic behaviors described by Brillouin functions.

IV. CONCLUSION

In summary, exact diagonalization studies of the magnetic properties of multiply charged II-VI CdSe nanocrystal quantum dots doped with few Mn^{2+} ions were presented. Remarkably, pronounced magnetic anisotropies are revealed in multiply charged symmetric NCQDs doped with few Mn^{2+} ions, which depend on electron number, Mn-ion distribution, and the strength of applied magnetic field. The magnetic anisotropies are attributed mainly to the magnetic-ion-induced orbital quenchings as a manifestation of the interplay between the discrete nature of Mn spin distribution and the electron-Mn spin interactions. The orbital quenchings associated with the ferromagnetic electron-Mn interactions further lead to significant suppression of magnetizations in the intermediate B regime. By contrast, the antiferromagnetic Mn-Mn interactions in the short-ranged Mn clusters result in substantially reduced magnetizations over a wide range of B. The combined effects of the orbital quenchings and the formation of Mn clusters lead to complex magnetic behaviors of randomly Mn^{2+}-doped colloidal quantum dots, which significantly deviate from the standard Brillouin-function descriptions.

ACKNOWLEDGMENTS

This work was supported by National Science Council of Taiwan under Contract No. NSC-95-2112-M-009-033-MY3. The author also would like to thank the National Center of Theoretical Sciences in Hsinchu and the National Center for High-Performance Computing of Taiwan for supporting.

[1] R. Beaulac, P. I. Archer, S. T. Ochsenbein, and D. R. Gamelin, Adv. Funct. Mater. **18**, 3873 (2008), and references therein.
[2] S. C. Erwin, L. Zu, M. I. Haftel, A. L. Efros, T. A. Kennedy, and D. J. Norris, Nature (London) **436**, 91 (2005), and references therein.
[3] F. V. Mikulec, M. Kuno, M. Bennati, D. A. Hall, R. G. Griffin, and M. G. Bawendi, J. Am. Chem. Soc. **122**, 2532 (2000).
[4] D. J. Norris, N. Yao, F. T. Charnock, and T. A. Kennedy, Nano Lett. **1**, 3 (2001).
[5] T. Ji, W. B. Jian, and J. Fang, J. Am. Chem. Soc. **125**, 8448 (2003).
[6] L. Besombes, Y. Leger, L. Maingault, D. Ferrand, H. Mariette, and J. Cibert, Phys. Rev. Lett. **93**, 207403 (2004); Y. Leger, L. Besombes, J. Fernández-Rossier, L. Maingault, and H. Mariette, *ibid.* **97**, 107401 (2006).
[7] J. I. Climente, M. Korkusinski, P. Hawrylak, and J. Planelles, Phys. Rev. B **71**, 125321 (2005).
[8] A. O. Govorov, Phys. Rev. B **70**, 035321 (2004); A. O. Govorov and A. V. Kalameitsev, *ibid.* **71**, 035338 (2005).
[9] A. K. Bhattacharjee and J. Perez-Conde, Phys. Rev. B **68**,

045303 (2003).
[10] F. Qu and P. Hawrylak, Phys. Rev. Lett. **95**, 217206 (2005); **96**, 157201 (2006).
[11] F. Qu and P. Vasilopoulos, Phys. Rev. B **74**, 245308 (2006).
[12] K. Chang, S. S. Li, J. B. Xia, and F. M. Peeters, Phys. Rev. B **69**, 235203 (2004).
[13] A. L. Efros, M. Rosen, and E. I. Rashba, Phys. Rev. Lett. **87**, 206601 (2001).
[14] I. Savic and N. Vukmirovic, Phys. Rev. B **76**, 245307 (2007).
[15] J. Fernandez-Rossier and L. Brey, Phys. Rev. Lett. **93**, 117201 (2004).
[16] R. M. Abolfath, P. Hawrylak, and I. Zutić, Phys. Rev. Lett. **98**, 207203 (2007).
[17] S. J. Cheng, Phys. Rev. B **72**, 235332 (2005); **77**, 115310 (2008).
[18] S. J. Cheng and P. Hawrylak, EPL **81**, 37005 (2008).
[19] N. T. T. Nguyen and F. M. Peeters, Phys. Rev. B **78**, 245311 (2008); **78**, 045321 (2008).
[20] R. M. Abolfath, A. G. Petukhov, and I. Zutić, Phys. Rev. Lett. **101**, 207202 (2008).
[21] I. Sarkar, M. K. Sanyal, S. Takeyama, S. Kar, H. Hirayama, H. Mino, F. Komori, and S. Biswas, Phys. Rev. B **79**, 054410 (2009).
[22] W. B. Jian, J. Fang, T. Ji, and J. He, Appl. Phys. Lett. **83**, 3377 (2003).
[23] A. D. Lad, Ch. Rajesh, M. Khan, N. Ali, I. K. Gopalakrishnan, S. K. Kulshreshtha, and S. Mahamuni, J. Appl. Phys. **101**, 103906 (2007).
[24] D. M. Hoffman, B. K. Meyer, A. I. Ekimov, I. A. Merkulov, Al. L. Efros, M. Rosen, G. Couino, T. Gacoin, and J. P. Boilot, Solid State Commun. **114**, 547 (2000).
[25] N. Feltin, L. Levy, D. Ingert, E. Vincent, and M. P. Pileni, J. Appl. Phys. **87**, 1415 (2000).
[26] S. Delikanli, S. He, Y. Qin, P. Zhang, H. Zeng, H. Zhang, and M. Swihart, Appl. Phys. Lett. **93**, 132501 (2008).
[27] J. K. Furdyna, J. Appl. Phys. **64**, R29 (1988).
[28] H. Ohno, D. Chiba, F. Matsukura, T. Omiya, E. Abe, T. Dietl, Y. Ohno, and K. Ohtani, Nature (London) **408**, 944 (2000).
[29] T. Dietl, Semicond. Sci. Technol. **17**, 377 (2002), and references therein.
[30] T. Jungwirth, J. Sinova, J. Masek, J. Kucera, and A. H. MacDonald, Rev. Mod. Phys. **78**, 809 (2006).
[31] U. Banin and O. Millo, Annu. Rev. Phys. Chem. **54**, 465 (2003).
[32] Y. Z. Hu, M. Lindberg, and S. W. Koch, Phys. Rev. B **42**, 1713 (1990).
[33] A. K. Bhattacharjee and C. Benoit a la Guillaume, Phys. Rev. B **55**, 10613 (1997).
[34] *Magnetism in Condensed Matter*, edited by S. Blundell (Oxford University Press, New York, 2001), Chap. 2.
[35] According to Hund's rules (Ref. 34), the total angular momenta of interacting $N_e=1,2,\ldots,8$ electrons successively filling the s and p shells follow the sequence $l=0$, 0, 1, 1, 0, 1, 1, and 0.